Hydrodynamics of long jet impingement

M. M. Seraj & M. S. Gadala
Department of Mechanical Engineering, University of British Columbia, Canada

Abstract

A circular turbulent long jet has been assessed numerically using the volume-of-fluid method to examine the hydrodynamics of a long jet before impingement and to inspect the flow structure of a radial thin layer spreading over a flat plate after impingement. Typical steel mill industrial parameters are used in the model. Comparative results are shown for laminar and turbulent jets with different turbulence models. Model results showed good agreement with the analytical solution available for global parameters and jet behaviour. The film thickness of the water layer over the plate, for more than 27 jet diameter, was measured by tracking free-surface. A hydraulic jump was detected and occurred within the radial zone in different shapes in laminar and turbulent modelling, respectively.

Keywords: hydrodynamics, long jet, numerical simulation, hydraulic jump.

1 Introduction

Jet impingement is one of the effective means in cooling and heating applications. Water jet impingement has a distinguished ability to dissipate a large amount of heat fluxes and has attracted many studies over the past few decades. Recent reviews may be found in [1–3].

In an axisymmetric jet, the jet thickness decreases as the liquid radially travels outward. The thickness of the liquid sheet initially decreases with the radius but, because viscous drag slows the liquid sheet, its thickness begins to increase at larger radii. The rapid thickness decrease brings the growing boundary layer into contact with the free-surface of the liquid layer. If the Reynolds number is large enough, a shift to a turbulent regime could be expected for the radially spreading thin laminar liquid film. Layer thickening after thinning marks the radius of transition [3, 4].

WIT Transactions on Engineering Sciences, Vol 59, © 2008 WIT Press
www.witpress.com, ISSN 1743-3533 (on-line)
doi:10.2495/AFM080351

Far downstream, the impinging jet flow may be terminated by a hydraulic jump whose location depends on both upstream and downstream flow conditions. The liquid layer thickness upstream from the hydraulic jump is necessary in order to determine the location of the hydraulic jump. This thickness is also used to find the Fraud number of magnitude [5]. The effect of gravity in a long jet causes speeding up of the jet and contracting of the jet diameter. For the long jet, turbulence has enough time to develop and it derives surface jet disturbances and jet splattering.

This paper discusses the numerical simulation of the hydrodynamics of an axisymmetric long jet impingement with typical industrial parameters. The jet is considered fully developed turbulent. The FLUENT program is used for the numerical modelling [6].

1.1 Geometry and jet parameters

The parameters used are: nozzle radius, 19 mm, nozzle height above plate, 1.5 m, and jet flow rate, 15 lit/sec. The height of the issuing jet, H, at a given time, t, may be obtained from the following simple analytical equation:

$$H = \frac{1}{2} g t^2 + v_j t \tag{1}$$

where g is the gravitational acceleration and v_j is the jet issuing velocity (nozzle exit velocity). At a given time, the velocity of the jet, v, and the jet diameter, d, may be obtained from the following relations:

$$v = \sqrt{v_j^2 + 2gH}\,, \qquad d = d_j \sqrt{\frac{v_j}{v}} \tag{2}$$

where d_j is the nozzle diameter. Table 1 shows the jet parameters used in the simulation (note that suffix '*imp*' stands for the impingement instant).

2 Numerical simulation

The problem has two very different length scales, which make the numerical simulation quite difficult and time consuming to model in one simulation. Therefore, the domain was divided into two parts as shown in fig. 1. The upper part extends from the nozzle to just above the plate surface (1.2 m long) and the lower part covers the impingement area and the plate surface. Outputs of the upper domain such as velocity and VOF profiles at the outlets of the upper domain are used as the input conditions (inlet boundary conditions) for the lower domain.

The domains discretized based on the finite volume method. The volume-of-fluid method (VOF) was employed to analyze this two-phase flow problem and to track the interface between the water jet surface and the surrounding air. Numerical simulations were carried out using the FLUENT program.

The assessment of film flow structure travelling over the plate was carried out by examining the distribution of VOF and the velocity along lines parallel to the plate at different heights above the plate. These lines are termed 'parallel lines' and they are 0.5 mm apart, therefore, a '*1 mm parallel line*' indicates a line parallel to the plate at a distance 1 mm above the surface.

3 Results

Along a parallel line, a VOF value of zero means pure air and a VOF value of 1.0 denotes pure water. Hence, a map of the measured VOF along parallel lines represents how the water sheet evolves at the top of plate and one could resolve reasonably the free-surface. The velocity profile inside the water and at free-surface could be drawn from the velocity distribution along parallel lines.

3.1 Laminar modelling

An experimental facility has been established at The University of British Columbia for testing the heat transfer and hydrodynamic behaviour of jet impingement on hot plates (see fig. 2).

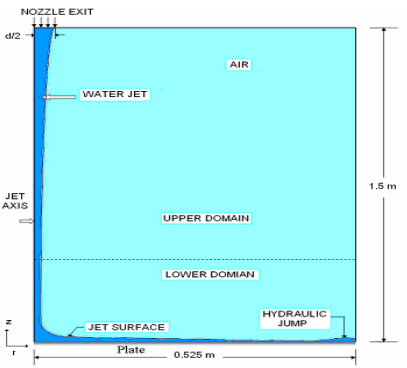

Figure 1: Problem geometry and jet parameters.

Table 1: Jet parameters.

r_j (mm)	19
V_j (lit/min)	15
V_j (m/s)	0.8817
V_{imp} (m/s)	5.5
r_{imp} (mm)	7.6
Re	33337
We	405

Experimental observations showed that the incoming jet is turbulent. Our simulation starts, however, with a laminar case just to establish some experience with the model. Table 2 shows the velocity and height data of the tip of the jet travelling downward until impingement in a laminar modelling. The subscript '*comp*' indicates FLUENT's results which is compared to results obtained from eqns. (1) and (2). Shortly after exiting the nozzle, the jet height resulted from the numerical simulation retarded by 10–20%. However, as time elapsed, the discrepancy decreased to less than 10%. In the lower domain the jet is generally off by less than 5% and the discrepancy is only about 2% near the plate surface. It should be noted that at a given time instant, the heights calculated analytically are larger than those calculated numerically indicating slightly faster velocities for the analytical solution. This is the case for both domains of analysis as indicated in table 2.

Fig. 3 shows the measured VOF distribution along a 0.5 mm parallel line. The measured VOF is 1.0 for the initial part of the line inside the stagnation zone. As the flow enters the radial zone, the water layer is thinned and the VOFs decreased. The assessment of VOF for a 0.2 mm parallel line shows that the film

has the thickness of 0.2–0.5 mm at the early region outside the stagnation zone (note that for the laminar simulation closer parallel lines are used just above the plate surface). A wavy free-surface was seen until a radius of more than 0.1 m was reached. Thereafter the film thickness was nearly unchanged but beyond the radius of 0.2 m the layer thickens. The parallel line is completely inside the water over the radius of 0.4 m.

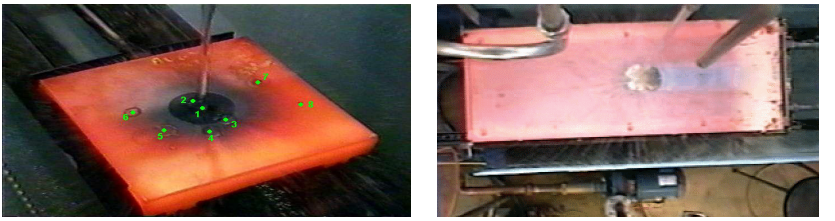

Figure 2: Experimental testing of stationary and moving plates.

Table 2: Height and velocity of laminar jet before striking the plate (a) upper domain, (b) lower domain.

(a)

time (sec)	**H** (m)	$\mathbf{H}_{com\ p}$ (m)	**V** (m/s)	$\mathbf{V}_{comp}$ (m/s)
0.05	**0.056**	**0.047**	**1.3**	**1.23**
0.12	**0.176**	0.16	**1.98**	**1.9**
0.2	**0.373**	0.34	**2.73**	**2.6**
0.275	**0.613**	0.58	**3.49**	**3.26**
0.344	**0.884**	**0.805**	**4.07**	**3.9**
0.4	**1.138**	**1.038**	**4.6**	**4.43**
0.425	**1.261**	**1.151**	**4.83**	**4.66**
0.433	**1.3**	**1.19**	**4.91**	**4.74**
0.435	**1.31**	**1.2**	**4.93**	**4.76**

(b)

time (sec)	**H** (m)	$\mathbf{H}_{com\ p}$ (m)	**V** (m/s)	$\mathbf{V}_{comp}$ (m/s)
0.004	**0.02**	**0.01**	**4.935**	**4.93**
0.025	**0.126**	**0.118**	**5.145**	**5.09**
0.035	**0.178**	**0.172**	**5.247**	**5.19**
0.045	**0.231**	**0.227**	**5.349**	**5.27**
0.055	**0.285**	**0.281**	**5.446**	**5.36**
0.0575	**0.299**	**0.295**	**5.472**	**5.374**
0.0578	**0.3**	**0.297**	**5.475**	**5.37**
0.058	**0.302**	**0.298**	**5.477**	**5.36**
0.0585	**0.304**	**0.3**	**5.481**	**0**

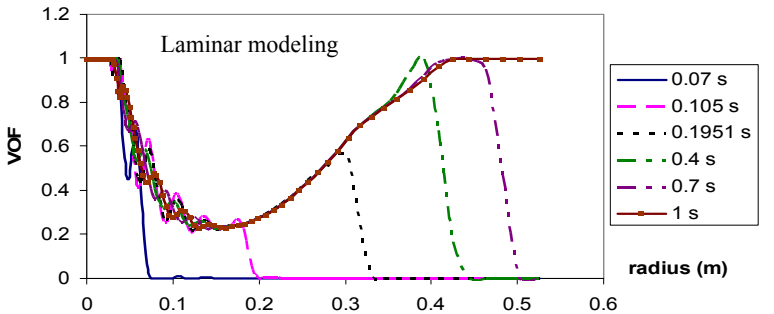

Figure 3: VOF distribution along a 0.5 mm parallel line.

A circular wave was seen at the leading edge of the water layer. The radial progress of the peak of the circular wave over the plate may be tracked by looking at the VOF variation along the higher parallel lines. At 0.4 sec the peak was well above 1 mm and thickness values become larger.

Fig. 4 shows the variation of radial velocity along a 0.5 mm parallel line. The velocities were decreasing monotonically as the fluid expanded radially downward. The numerically detected velocity fluctuations correspond to a wavy free-surface outside the stagnation zone as the liquid sheet thinned. The velocity ultimately became negligible at the plate border (over the radius of 0.5 m).

The assessment of radial velocity for lines parallel to the plate surface at different heights from the plate (up to 4 mm) revealed that the water film velocity has very similar variations along these lines, such as those shown in Figure 4. This result is quite reasonable and expected because of thinning of the water layer.

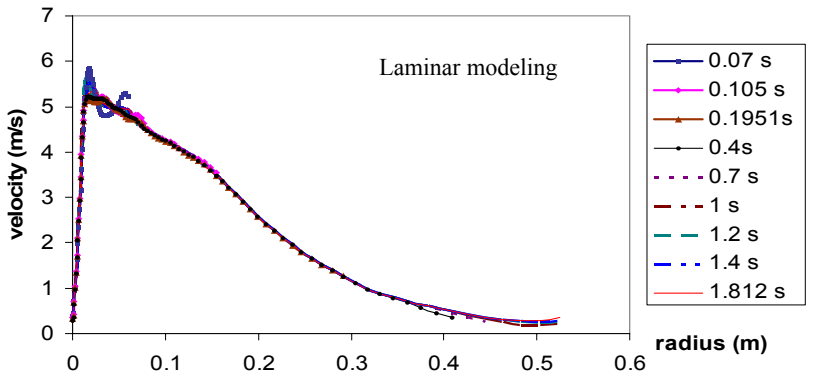

Figure 4: Velocity along a 0.5 mm parallel line.

3.2 Turbulent simulation

3.2.1 k-ε turbulent model

Table 3 shows the data of velocities and heights of the jet tip during impinging from the nozzle for different times until impingement on the plate using the k-ε turbulent model with wall functions. This model shows better performance for a radial jet with strong streamline curvature because it is adapted for wall bounded flows [6]. Analytical results could be determined as mentioned above in the laminar case. In the upper analysis domain, the differences between these results and the analytical ones are 5%. The difference in jet development in lower domains is about 10–20% showing a faster analytical jet from the analytical results by about 10%. The numerical simulation was continued until the jet passed the outlet of the lower domain and until striking the plate in the lower domain.

Fig. 5 shows the measured VOF along a 0.5 mm parallel line. Thinning of the water layer is evident as it exits the stagnation zone and free-surface disturbances have been determined for a radius of up to 0.1 m. Thereafter, the water layer

thickness starts to increase while the free-surface disturbances continue to more than 0.2 m radius. After 0.3 m the film thickness is more than 0.5 mm and parallel lines at larger distance from the plate are needed to assess the wavy free-surface. The VOF assessment for the parallel lines up to 5 mm show that the water layer thickness could rise up to 4.5 mm.

Radial velocity distribution along a 1 mm parallel line is shown in fig. 6. Also, each line shows how much the fluid is widening over the plate as time elapses until water covers the plate. The flow has velocity parallel to the plate after impinging almost equal to the incoming jet velocity. After exiting the

Table 3: Height and velocity of jet before striking the plate for k-ε model (a) upper domain, (b) lower domain.

(a)

time (sec)	H (m)	H_{comp} (m)	V (m/s)	V_{comp} (m/s)
0.05	0.056	0.049	1.32	1.28
0.12	0.176	0.166	2.0	1.95
0.2	0.373	0.349	2.76	2.64
0.275	0.61	0.571	3.46	3.34
0.35	0.91	0.845	4.166	4.05
0.395	1.11	1.036	4.6	4.46
0.413	1.2	1.119	4.77	4.64
0.42	1.24	1.149	4.83	4.69
0.424	1.26	1.166	4.86	4.74
0.431	1.29	1.2	4.93	4.82

(b)

time (sec)	H (m)	H_{comp} (m)	V (m/s)	V_{comp} (m/s)
0.004	0.0197	0.01	4.935	4.75
0.025	0.126	0.104	5.12	4.8
0.035	0.178	0.153	5.21	4.9
0.045	0.231	0.203	5.3	4.95
0.055	0.2852	0.253	5.4	5.08
0.0606	0.316	0.283	5.45	5.18
0.063	0.329	0.2953	5.47	5.1
0.064	0.333	0.3	5.48	0

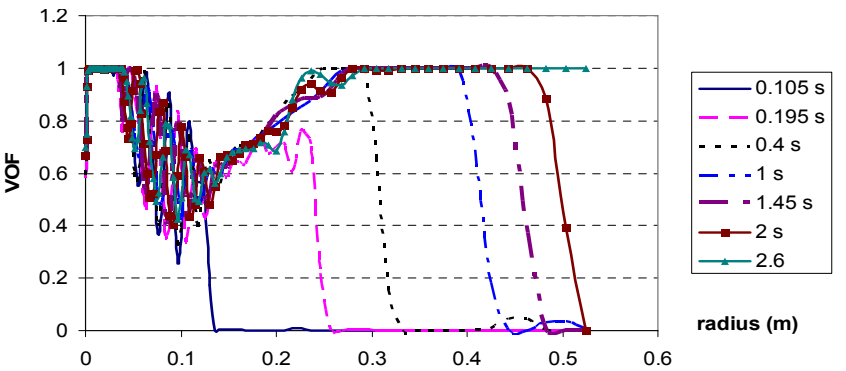

Figure 5: VOF distribution along a 0.5 mm parallel line.

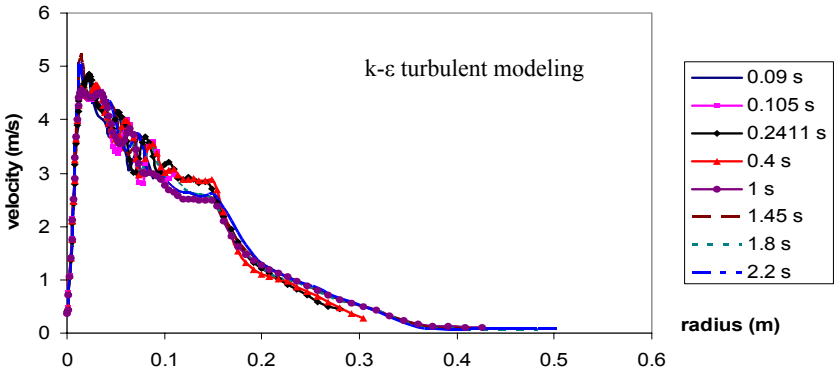

Figure 6: Velocity along 1 mm parallel line.

Table 4: Height and velocity of the jet before impacting the plate for the k-ω model: (a) upper domain (b) lower domain.

(a)

time (sec)	H (m)	H_{comp} (m)	V (m/s)	V_{comp} (m/s)
0.05	0.056	0.0472	1.32	1.19
0.107	0.151	0.132	1.835	1.77
0.2	0.373	0.337	2.76	2.6
0.275	0.614	0.557	3.47	3.27
0.35	0.91	0.825	4.119	4.0
0.4	1.137	1.0345	4.59	4.45
0.413	1.2	1.095	4.93	4.58
0.424	1.256	1.143	4.82	4.68
0.43	1.287	1.172	4.87	4.74
0.433	1.30	1.186	4.904	4.78
0.436	1.314	1.2	4.93	4.81

(b)

time (sec)	H (m)	$H_{com\ p}$ (m)	V (m/s)	V_{comp} (m/s)
0.004	0.0197	0.01	4.94	4.79
0.015	0.0748	0.065	5.04	4.8
0.025	0.126	0.115	5.14	4.93
0.035	0.178	0.164	5.23	5.02
0.045	0.231	0.213	5.32	5.19
0.05	0.258	0.239	5.37	5.18
0.060	0.316	0.296	5.47	5.23
0.061	0.319	1.5	5.48	0

stagnation zone, the velocity is reduced while water expands in the radial zone downstream but has some fluctuations extending over a radius of 0.1 m. The velocity became flat thereafter and then dramatically decreased as the film thickness increased.

3.2.2 k-ω modelling

Table 4 shows the velocities and the heights of the jet tip during impinging from the nozzle exit and up to the impingement on the plate surface in the turbulent case using the shear stress transport (SST) k-ω model. This model has better performance than the standard k-ε model. The analytical results could be found as mentioned in the laminar case. The numerical results show jet delays from analytical one in the upper domain by 10% except for earlier times while the velocities are lower than the analytical results by less than 5%. In the lower domain, the comparison gives similar results as the upper domain.

Fig. 7 shows the development of water over the plate by the variation of measured VOF along a 0.5 mm parallel line. The peaks of VOFs were decreasing while the liquid spread beyond the radius of 0.1 m. However the trend turned over and the peaks began to increase. Enhanced water layer thickness reached the 1 mm parallel line at a time of around 0.4 sec and then passed it. The evaluation of other higher parallel lines reveals that the maximum height ultimately became larger than 3.5 mm. The evaluation of the velocity of the spreading water sheet at the top of the surface could also be discerned. In the stagnation zone downstream, as the thickness reduced the velocity fluctuations were seen to be monotonically decreasing.

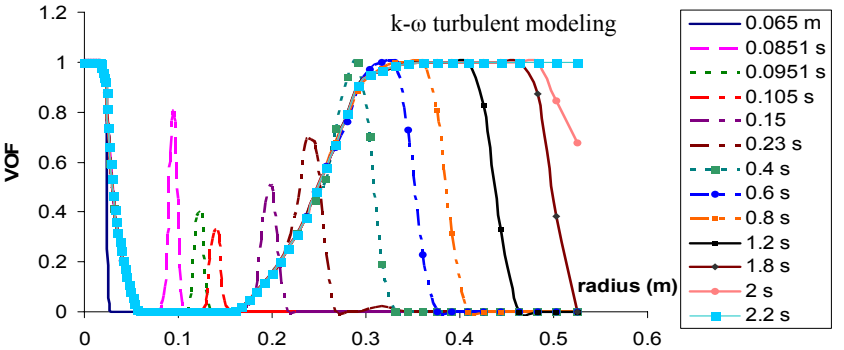

Figure 7: VOF distribution along a 0.5 mm parallel line.

4 Splashing

The exiting jet from the nozzle is fully developed turbulent which makes the jet surface rough on contact with the air and ultimately causes disturbances in the jet surface coming vertically toward the plate. A jet surface disturbance for turbulent modelling using k-e in the lower domain is shown in fig. 8. Any turbulence in the incoming axisymmetric jet can significantly disturb the free-surface of the thin liquid sheet, causing splattering of the liquid advancing parallel to the plate.

Bhunia and Lienhard [7] and Lienhard et al [8] developed a model for splattered fully developed turbulent jets. The onset of splattering where 5% of the incoming fluid is splattered is [7]:

$$\frac{S_0}{d_j} = \frac{130}{1 + 5 \times 10^{-7} We_d^2} \tag{3}$$

$$W_{e_d} = \rho v_j^2 d_j / \sigma \tag{4}$$

where W_e is Weber number.

This gives S0/dj ≈120 which is quite different from S/dj ≈ 40 obtained in this problem. Therefore, we expect to have less than 5% splashing while the jet travels downward. In the actual numerical simulation, we were able to capture a few ejecting drops from the jet tip in our turbulent simulation by reasonably fine mesh in the upper domain (fig. 8). This jet has a low Weber number. Therefore, the surface tension effect is dominant but it doesn't capillary break up [7].

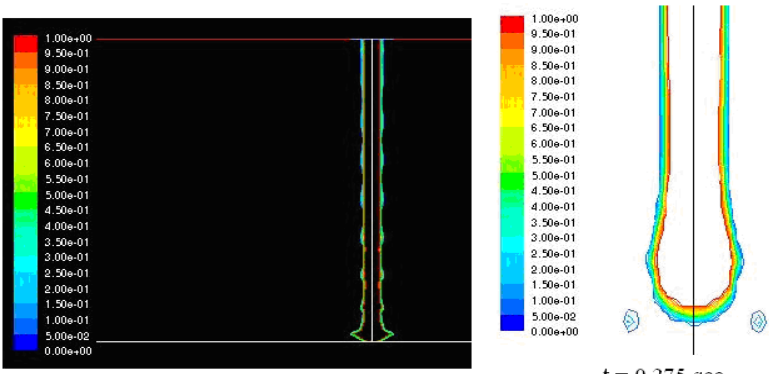

Figure 8: (a) jet surface disturbances; (b) drop splashing.

In k-ω turbulent modelling, the measured VOF of between 0 and 1 was found in some cells outside (above) the free-surface which may be an indication for splattering after impingement; tiny water drops in the air need highly refine mesh to confirm.

5 Discussion

In the laminar simulation case, the assessment of free-surface was carried out by measuring the VOF along the parallel lines up to 5 mm. The water film thickness covering a large area of the plate is extremely thin (0.2–0.5 mm). As the circular wave passes, the thickness h increases and then decreases again. The maximum thickness was detected with a value over 2 mm at the peak of the circular wave.

The radius of transition from laminar to turbulent was found to be around 0.2 m [2]. The wavy free-surface of this thin layer could be related to the eddies inside the layer [4]. It was not possible to measure the turbulent parameters in laminar modelling in FLUENT to confirm the position of transition to turbulent flow but increasing the thickness layer may be considered as an indication for this change [9]. The size of the plate is over 20 jet diameters and the flow has the Fraud number above 2, which are good indications for the occurrence of a hydraulic jump in a circular jet [4]. Therefore, considering the circular wave as a hydraulic jump, then it is a jump with a roller that could be unstable [5].

The free-surface was examined by measuring the VOF along the parallel lines up to 5 mm for k-e modelling. The free-surface disturbances were seen downstream of the stagnation zone which extend to around r = 0.1 m. The film became very thin and the height monotonically decreased to less than 0.5 mm. Thereafter, the thickness was increasing up to more than 4.5 mm.

The results for k- ω modelling are similar to k-ε but the maximum height is up to 4.5 mm. The water expanded over the target in a smoother layer than using k-ε model. Beyond 0.2 m in radius, the thickness of the front of the film started to increase with negligible radial velocity. This may be considered an indication

for the occurrence of a hydraulic jump. The shape of a hydraulic jump in turbulent modelling is a curve without a roller, which differs from the jump in the laminar case. The obtained results for turbulent modelling of a jet are better than those for the laminar one before impingement because higher order schemes for momentum equation and turbulent equations were chosen and finer mesh is used. However, in the laminar case the film was spreading faster than in the turbulent situations at the top of the plate and becoming thinner.

Watson [10] presented a model to determine the radius of the hydraulic jump for a radial spreading liquid layer without considering the jump width. Agreement with experimental data has been mixed [2]. Simple calculations reveal that the hydraulic jump could be occurring in laminar case [11]. Based on the assessment of the numerical results, a thickness of 1.5–2.5 mm was considered to have a crude estimate for the radius of the hydraulic jump using the Watson model in the laminar case. The jump radius was obtained in the range of 0.1–0.2 m, which is consistent with what has been shown in Figure 2. Free-surface disturbances need more mesh refining to be reasonably resolved, especially when a wavy surface is evident as is the case in the above simulations. Near the wall region, up to 4 mm for laminar and up to 6 mm for turbulent, should also be refined more.

References

[1] Viskanta, R., and Incropera, F. P., Quenching with liquid jet impingement. In Heat and Mass Transfer in Materials Processing, I. Tanasawa and N. Lior, eds., Hemisphere, New York, pp. 455–476, 1992.

[2] Lienhard, J.H., "Liquid jet impingement", in Annual Review of Heat Transfer, pp. 199–270, 1995.

[3] Webb, B.W. and Ma, C.-F., "Single-phase liquid jet impingement heat transfer", Advances in Heat Transfer, 26, pp. 105–217, 1995.

[4] T. Azuma and T. Hoshino, The Radial Flow of a Thin Liquid Film (Laminar Turbulent Transition), Bull. ISME, 27, pp. 2739–2746, 1984.

[5] X. Liu and J. H. Lienhard V, The Hydraulic Jump in Circular Jet Impinge-ment and in other Thin Liquid Films, Exp. Fluids, 15, pp.108–116, 1993.

[6] FLUENT 6.3 User's Guide

[7] S. K. Bhunia and J. H. Lienhard V, Splattering during Turbulent Liquid Jet Impingement on Solid Targets, J. Fluids Eng., 116, pp. 338–344, 1994.

[8] Lienhard, J. H. V., Liu, X., and Gabour, L. A., Splattering and heat transfer during impingement of a turbulent liquid jet. *J. Heat Transfer* 114, 362–372, 1992.

[9] T. Azuma and T. Hoshino, The Radial Flow of a Thin Liquid Film (2nd Report, Liquid Film Thickness), Bull. JSME, Vol. 27, pp. 2747–2754, 1984.

[10] B. J. Watson, The Radial Spread of a Liquid Jet over a Horizontal Plane, J. Fluid Mech., 20, pp. 481–99, 1964.

[11] M. Errico, A Study of the Interaction of Liquid Jets with Solid Surfaces, Ph.D. Dissertation, Univ. of California at San Diego, San Diego, CA, 1986.